Laser induced fluorescence study of the $\tilde{B}\,^2A'' \rightarrow \tilde{X}\,^2A''$ transition of the vinoxy radical in a supersonic free jet expansion

L. F. DiMauro, M. Heaven,[a] and Terry A. Miller
AT&T Bell Laboratories, Murray Hill, New Jersey 07974

(Received 25 April 1984; accepted 16 May 1984)

The vinoxy, CH_2CHO, free radical has been produced in a supersonic free jet expansion by ArF excimer laser photolysis of a suitable precursor like ethyl vinyl ether. Electronic spectra involving the $\tilde{B}\,^2A'' \leftrightarrow \tilde{X}\,^2A''$ transition have been observed at vinoxy temperatures between 2–30 K. Rotational structure as well as spin splittings have been resolved. Analysis of the spectrum yields the electronic term value, vibrational frequencies, rotational and spin-splitting constants for both electronic states. These molecular parameters provide considerable information about the electronic and geometric structure of the radical.

I. INTRODUCTION

Simple alkoxy radicals are of considerable importance. From a practical point of view, they are known to play important roles in combustion processes and photochemical air pollution. The C_2H_3O molecule is the prototype alkenyloxy radical and experiments indicate that it is a primary product of the $O(^3P) + C_2H_4$ reaction.[1,2]

From a theoretical point of view, it is a most interesting system, which has been the object of several recent *ab initio* calculations.[3–5] Figure 1 shows the three lowest energy valence bond structures of the C_2H_3O radical, which for simplicity we shall refer to as vinoxy. As Fig. 1 indicates the energy ordering of the various states is very sensitive to the details of the calculation. While there is little doubt that the CI calculation gives the best description of the vinoxy radical, the extreme sensitivity of the calculation to basis set clearly indicates a strong need for detailed experimental results for vinoxy in order to test the absolute accuracy of any *ab initio* calculation.

There have been several recent experimental observations of the vinoxy radical. Hunziker *et al.*[6] detected CH_2CHO using kinetic absorption spectroscopy. Laser induced fluorescence (LIF) detection of vinoxy was accomplished by Inoue and Akimoto[7] in a fast flow system. Jacox observed IR spectra of vinoxy in an Ar matrix.[8] Later Kleinermanns and Luntz[1] used LIF to detect product CH_2CHO in crossed molecular beams reactions. Of the various optical experiments, only the one of Inoue and Akimoto gave much spectroscopic information. They reported and assigned vibrational structure in both the excitation spectrum and in the laser excited, wavelength resolved emission spectrum. They were able to obtain approximate frequencies for the three skeletal vibrational modes in both the ground and excited states of vinoxy.

There has never been any rotational structure resolved in the spectrum of CH_2CHO. At least in the experiments of Inoue and Akimoto, this was largely due to the highly congested rotational structure present at ambient temperature. To obtain a rotationally resolved spectrum of CH_2CHO, which is analyzable, we have produced very cold vinoxy. This was accomplished by the ArF photolysis of ethyl vinyl ether entrained in a supersonic free jet expansion.

The fragment CH_2CHO initially contains considerable internal excitation. However, subsequent collisions with the jet's inert gas molecules cool the rotational degree of freedom to $\lesssim 5$ K. Such spectra are simple and easy to analyze. By translating the probe laser to a region where the cooling is less complete more complicated spectra involving more rotational levels can be observed. Since the molecular param-

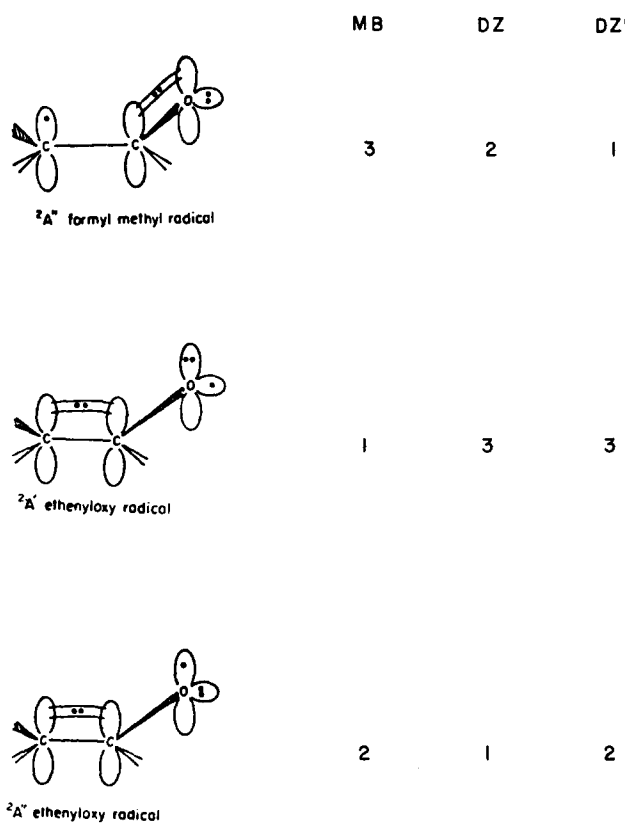

FIG. 1. The three lowest energy, valence bond structures of the vinoxy radical. The calculated order of their energies (1 = lowest, 3 = highest) is given to the right of each structure. The key to the calculations is MB = minimal basis set (STO-3G), DZ = double zeta, DZP = double zeta with polarization. Configuration interaction calculations mix strongly the two $^2A''$ states with the associated repulsion leaving the $^2A'$ state intermediate in energy. For more details of the calculations, see Dupris *et al.* (Ref. 3).

[a] Present address: Department of Chemistry, Illinois Institute of Technology, Chicago, IL 60616.

 0021-9606/84/172339-08$02.10

eters are already approximately known from the analysis of the very cold spectra, the somewhat warmer, somewhat more complicated spectra also yields fairly easily to analysis.

From our analysis we obtain values for the three rotational constants A, B, and C for both the ground $\tilde{X}\,^2A''$ and excited $\tilde{B}\,^2A''$ states in the observed transition. We obtain an accurate term value T_{00} for the transition. We are also able to resolve spin splittings in several rotational transitions, and therefore derive a value for the spin splitting parameter κ in both states. In addition, we have remeasured the origins of a number of the vibronic transitions both in the excitation spectrum and in the laser excited, wavelength resolved emission spectrum. We obtain improved values of the vibrational frequencies, which in some cases differed considerably from the earlier values reported by Inoue and Akimoto.[7] Overall our measurements provide a much needed experimental description of the structure of the $\tilde{X}$ and $\tilde{B}\,A''$ states of vinoxy.

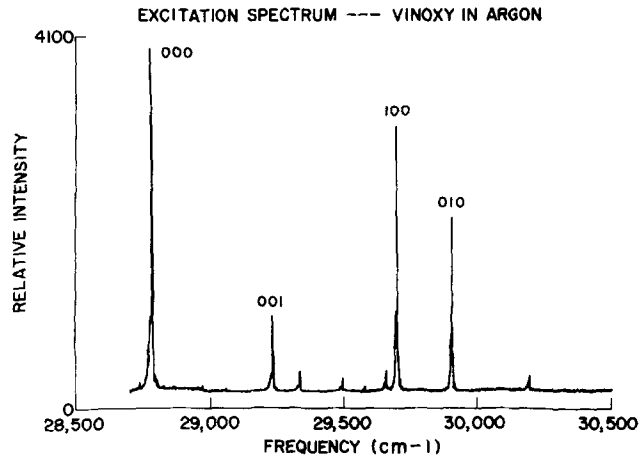

FIG. 2. Section of the free jet laser excitation spectrum of vinoxy. The transitions all originate in the vibrationless level of the $\tilde{X}$ state and the labels refer to the vibrational quantum numbers of the terminating level in the excited $\tilde{B}$ state.

II. EXPERIMENTAL

Details of the free jet expansion apparatus have been previously described.[9,10] Briefly, we utilize a continuous "Camparque" supersonic free expansion with a 250 μm diameter nozzle. Carrier gas stagnation pressures used for helium were 8–40 atm and for argon were 8–13 atm. The ethyl vinyl ether precursor was seeded in the carrier gas prior to expansion and introduced by flowing the carrier gas over the liquid which was held in a metal container at 0 °C. A lightly focused ArF* (193 nm) excimer laser (Lumonics 860-3) was used to produce the vinoxy radical. The ArF* laser intersected the expansion ~12 nozzle diameters (n.d.) downstream of the orifice.

The counter propagating LIF probe was a Molectron N_2 pumped dye laser which was frequency doubled producing ~10 μJ/pulse of tunable radiation from 330–350 nm. This beam probed the expansion ~40 n.d. downstream of the orifice. The ~28 n.d. separation between the two lasers allowed ample time for the vinoxy radicals produced in the photolysis region to "cool" via two body collisions with the carrier gas. Laser excitation scans were obtained by collecting the total LIF on a EMI 9659QB photomultiplier tube, as the laser frequency is swept. The probe laser linewidth for the low resolution scans was ~0.8 cm^{-1}. To obtain rotational resolution, the dye laser was operated with an intracavity etalon, yielding a UV linewidth of ~0.06 cm^{-1}. The laser frequency was scanned by varying the pressure of either N_2 or SF_6 in the cavity from 0 to 1 atm. The excitation spectra were calibrated by simultaneously recording the optogalvanic spectrum of the U atom (low-resolution scans) or the LIF of I_2 (etalon scans) and referring to the respective atlases.[11,12]

The wavelength resolved spectra are recorded by pumping a particular vibrational transition with the probe laser frequency fixed and dispersing the LIF through a 0.32 m, $f/4.2$ monochromator. A PAR, Model 1420, OMA detector is utilized to view an ~250 Å spectral region in a single laser shot. The resolution of this system was ~2.5 Å. The scans were calibrated using Ne and Hg lamps and referring to standard tables.[13]

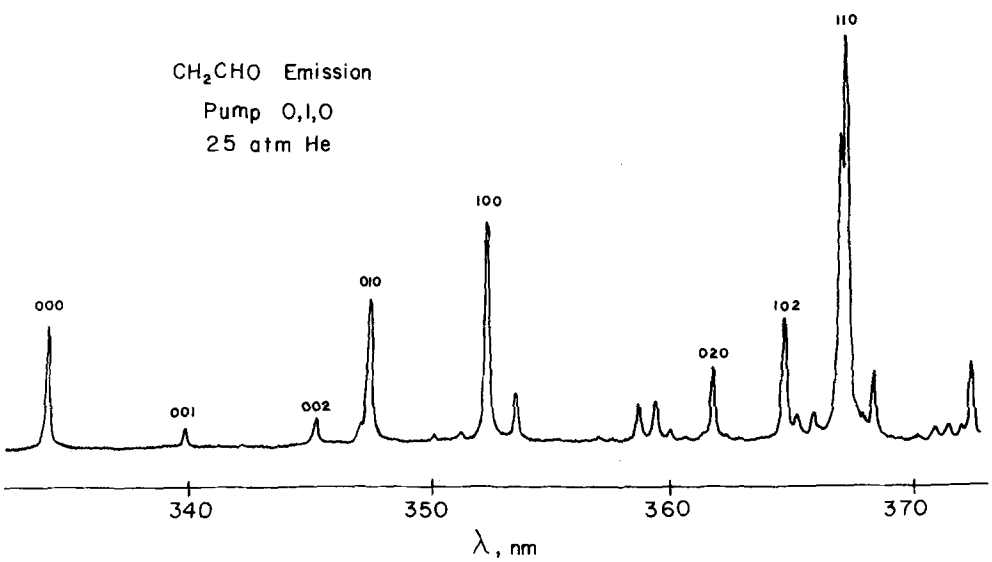

FIG. 3. Section of the free jet laser excited, wavelength resolved emission spectrum of vinoxy. Labels refer to vibrational quantum numbers of the terminating ground state level.

III. SPECTRAL ANALYSIS

A. Vibrational spectra

As mentioned in the Introduction the first LIF studies of vinoxy were by Inoue and Akimoto.[7] In their case the vinoxy radical was generated by chemical reaction in a fast flow system and observed at room temperature. They obtained vibrationally resolved excitation and laser excited wavelength resolved emission, spectra. These spectra, especially the excitation one, showed rotational contours, but no attempt was made to resolve rotational structure. Measurements were made of the positions of the peaks of the unresolved vibrational transitions, assignments made, and vibrational frequencies determined.

In Figs. 2 and 3, we show, respectively, the excitation and laser excited wavelength resolved emission spectra of vinoxy taken at low resolution in the free jet expansion. A comparison with Figs. 1 and 3 of the work of Inoue and Akimoto[7] shows a marked improvement in resolution, presumably because of the virtual elimination of rotational contours in the jet. Since this spectrum is so cold, the peak positions can properly be interpreted as band origins in the present spectra.

TABLE I. Fundamental frequencies in cm^{-1} of skeletal vibrations of vinoxy. Values in parentheses are from Ref. 7.

	ν_1	ν_2	ν_3
Excited state	917 (872)	1122 (1110)	450 (432)
Ground state	1540 (1560)	1143 (1150)	496 (530)

Following the lead of Inoue and Akimoto, we assign all the strong lines in both the excitation end emission spectrum to motions occuring mainly in the C–C–O skeleton. We label the transitions in terms of (ν_1,ν_2,ν_3), where roughly speaking[7] ν_1 is the C–O stretch, ν_2 in the C–C stretch, and ν_3 is the C–C–O bend. Table I gives our values for these three fundamental frequencies in both the ground and excited states. In parentheses are listed the corresponding values determined by Inoue and Akimoto. While some difference might be expected because we measure band origins and they measure bandheads, it is clear that in several cases the discrepancy between their and our values is much greater than would be

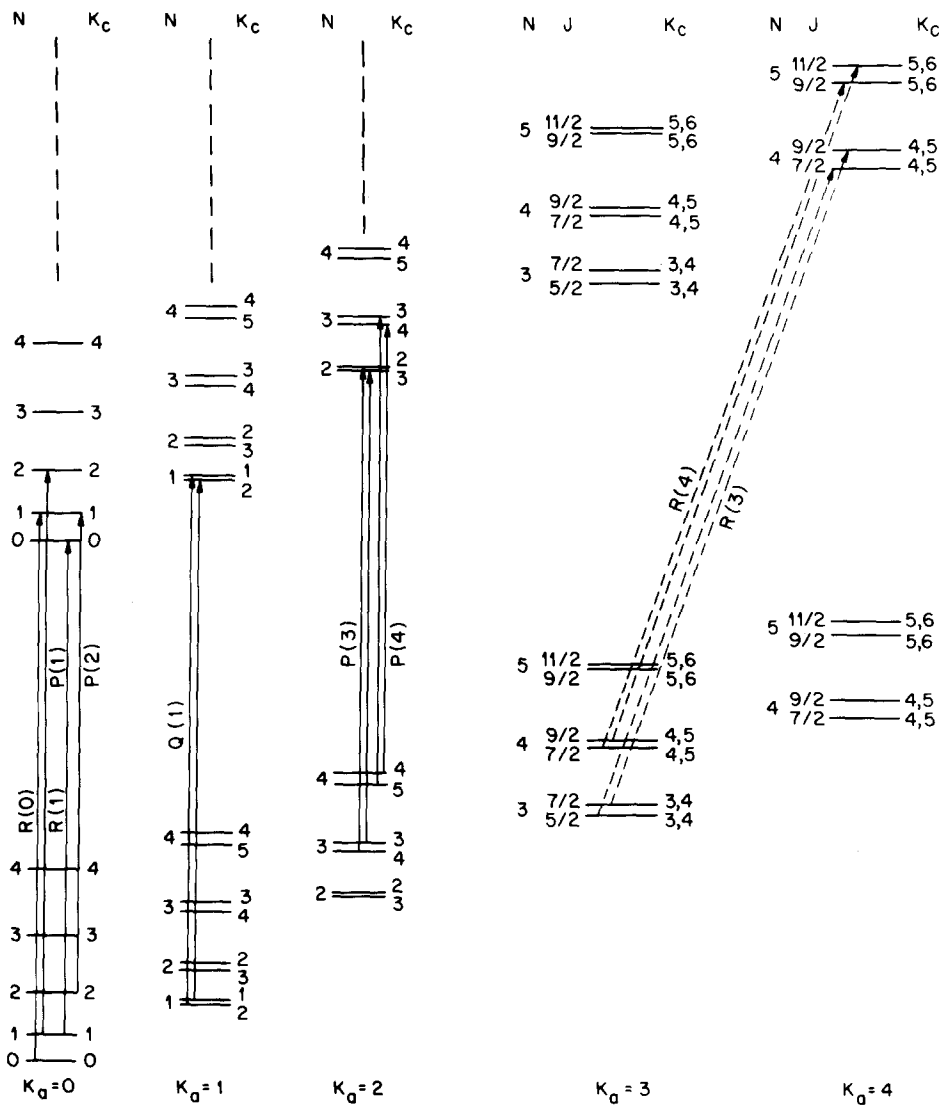

FIG. 4. Energy level diagram illustrating the rotational and fine structure in the electronic transition of a near prolate symmetric top in a doublet state. Both parallel (left) and perpendicular (right) transitions are illustrated. For the lower K_a levels, K splitting is illustrated, while for the higher K_a levels spin splitting is shown. This is consistent with the fact that spin splitting increases with K while K doubling decreases. Similarly the K splitting becomes unobservable for the high K_a levels.

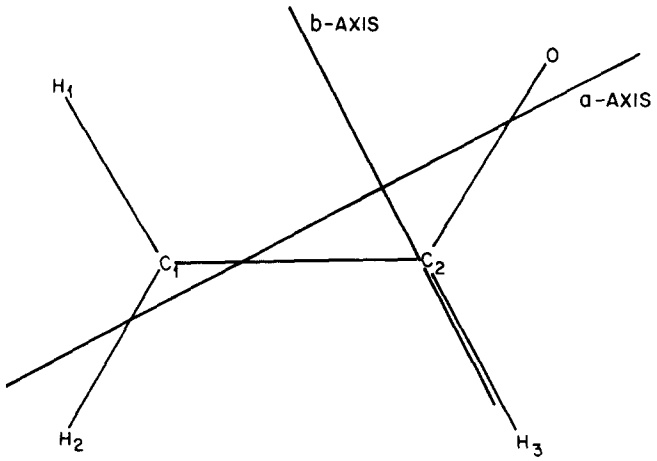

FIG. 5. Inertial axis for the vinoxy radical.

expected on this basis. We can offer no explanation, but do note that we have carefully checked our results and believe them to be accurate.

Generally speaking the techniques employed did not lend themselves easily to extensive data gathering on vibrational progressions. However, some comments can be made on the anharmonicity of two of the three ground state vibrations. Multiple results were obtained for ΔG_{1-0} and ΔG_{2-0} for ν_1 leading to values of $\omega_e = 1562\ \mathrm{cm}^{-1}$ and $\omega_e x_e = 10.5\ \mathrm{cm}^{-1}$, a modest anharmonicity. For the lower frequency ν_3 motion, we find $\omega_e = 534\ \mathrm{cm}^{-1}$ and $\omega_e x_e = 19\ \mathrm{cm}^{-1}$, considerably more anharmonic.

B. Rotational structure

The electronic spectrum of a molecule like vinoxy can be rather complicated when a high resolution spectrum is obtained. Figure 4 represents a general energy level diagram for an electronic transition of the type observed for vinoxy. Figure 5 shows the location of the inertial axes of vinoxy. Figures 6 and 7 show representative, rotationally resolved, spectra of the 0,1,0 band of the $\tilde{B}\,^2A'' - \tilde{X}\,^2A''$ transition of vinoxy.

Figure 5 was initially based on the *ab initio* calculation of Dupris *et al.*,[3] but in fact for the present purposes could have been roughly constructed from the known bond lengths and angles of similar compounds. Figure 5 shows that vinoxy is nearly a prolate symmetric top. Actual calculation (based upon the *ab initio* results) gives values of the asymmetry parameter κ of $\kappa'' = -0.94$ and $\kappa' = -0.92$. (For a prolate symmetric top with symmetry axis a, $\kappa = -1.0$.) For this reason, the energy levels of Fig. 4 approximate those of a prolate symmetric top.

As Fig. 4 shows there are a number of allowed transitions. On the left-hand side of Fig. 4, $\Delta K_a = 0$ parallel branch transition are illustrated, while on the right-hand side of Fig. 4, $\Delta K_a = 1$ perpendicular branch transitions are illustrated. The intensity of parallel transitions is dependent upon the transition dipole along the a axis while perpendicular transitions have their intensities determined by the component of the dipole along the b axis. If one makes the reasonable assumption that the dipole moment is mainly confined to the C–C–O skeleton, then it is clear from Fig. 5 that it lies nearly along the a axis with only a small component along the b axis. (In general, a dipole component along the c axis will also contribute to the perpendicular band's intensity, but both the *ab initio* calculation by Dupris *et al.*[3] and our subsequent analysis shows vinoxy to be a planar molecule to a very good approximation, so that the dipole component along the c axis vanishes.) Experimentally this suggestion is strongly confirmed with the perpendicular branches being an order of magnitude weaker.

Figure 6 shows the spectrum of vinoxy in the region of the parallel transition. The temperature of this spectrum is < 5 K so that only the lowest $K_a = 0$ levels have appreciable population. For the $K_a = 0$ level there is obviously no K doubling so that the rotational energy levels are well ap-

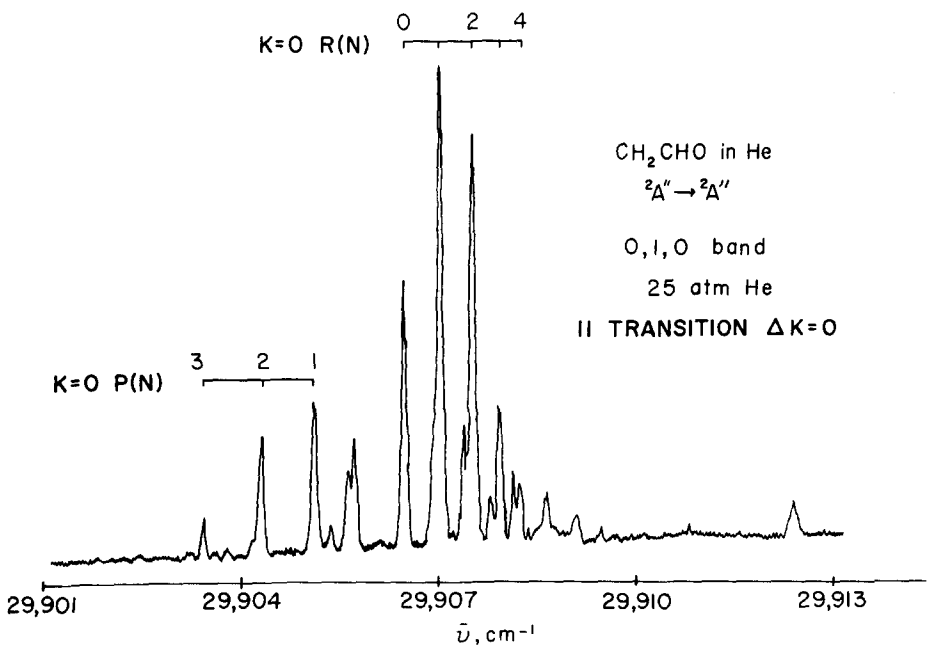

FIG. 6. Section of rotationally resolved spectrum of vinoxy in the region of the parallel transitions. The rotational temperature is between 2–3 K for the $K = 0$, N states. The relative populations of the different K levels must be described by a slightly higher temperature ~5 K.

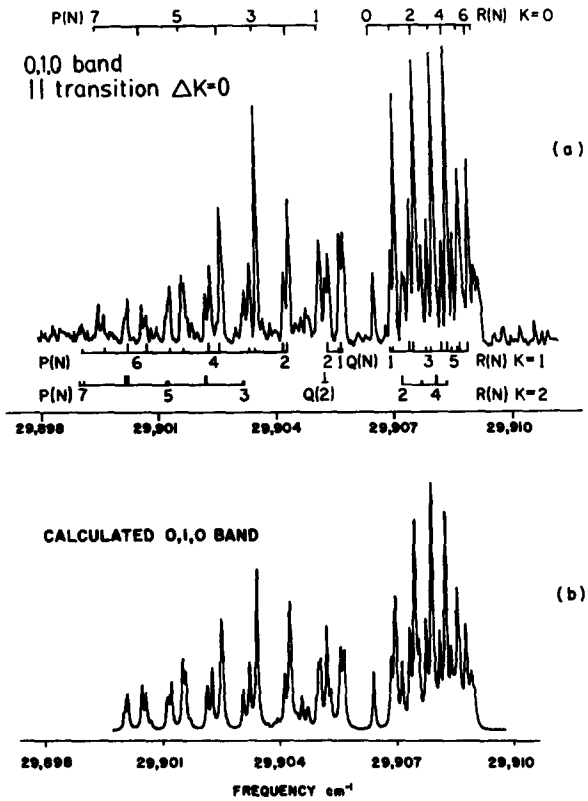

FIG. 7. (a) Spectrum of vinoxy covering approximately the same frequency region as Fig. 6, but with the rotational temperature now approximately 10 K, (b) a simulation of spectrum in (a) based upon the constants in Table II.

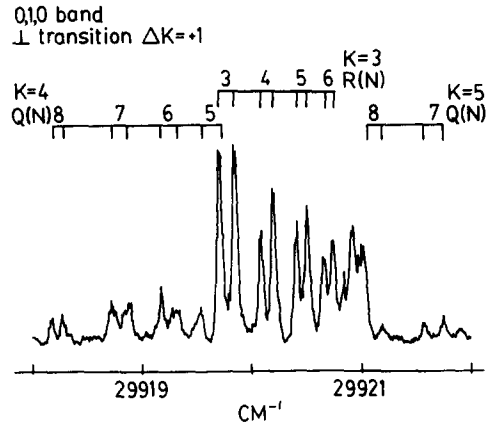

FIG. 8. Portion of the vinoxy spectrum showing $\Delta K_a = +1$ perpendicular transitions. Spin splitting of the rotational levels is evident here. To obtain these higher K_a level transitions the CH_2CHO is warmed to ~25 K.

proximated[14] by the simple prolate symmetric top formula

$$F(N) = \overline{B}N(N+1) + (A - \overline{B})K_a^2 \quad (1)$$

with $\overline{B} = \frac{1}{2}(B + C)$ and A, B, and C are the three rotational constants. Combination differences generated from Eq. (1) were used to confirm the initial R and P branch assignments done by inspection. The values of $\overline{B}'$ and $\overline{B}''$ obtained in this manner were used as initial estimates for later least square fits.

In the region between the $P(1)$ and $R(0)$ lines there are a group of lines which arise from the superpositions of Q-branch rotational transitions for which $K_a'' \geq 1$. The displacement of the Q branch lines give a crude estimate of $(\Delta A - \Delta\overline{B})$, but the data from perpendicular bands is required to obtain unique values for A' and A''.

In Fig. 7, the temperature of the spectrum has been raised to ~10 K by varying the jet conditions. The P and R branch $K_a = 0$ transitions identified in Fig. 6 are still the strongest lines in the spectrum; however, there are now several weaker lines associated with each of the $K_a \neq 0$ transitions. These weaker lines arise from transitions out of $K_a = 1$ and 2 levels which now are appreciably populated in the warmer jet. While Fig. 7 appears rather complex, the lines can be fairly readily assigned based upon the results from Fig. 6. In the case of the $K_a = 1$ and 2 levels, K doubling is clearly seen.

The perpendicular transitions give us the independent information needed for determination of the values of A' and A''. From Eq. (1) it can be shown that the energy difference between corresponding parallel and perpendicular ($\Delta K_a = +1$) rotational transitions originating in the same K_a'' level is just $(2K_a'' + 1)(A' - \overline{B}')$. Figure 8 shows several $\Delta K_a = +1$ transitions. (The $\Delta K_a = +1$ transitions are relatively easy to observe because the $\Delta K_a = 0$, R branch forms a head, so weak high N, R branch lines do not overlap the $\Delta K_a = +1$ transitions as high N, P branch transitions do with the $\Delta K_a = -1$ transitions.)

The lines in Fig. 8 are clearly split into doublets. One might first imagine that this splitting was caused by K doubling as is evidenced in Fig. 7. However, the magnitudes of the doublet splittings in Fig. 8 are clearly not consistent with the K doubling established in the parallel transitions. In fact, because the K doubling decreases as K increases,[14] the K doubling of the transitions in Fig. 8 should be completely unresolved within experimental linewidths. For this reason, we assign the doubling of the perpendicular transitions to spin splitting which we treat in detail in the next section. The spin splitting is a small perturbation and can be treated independently of the rest of the rotational analysis. For the rotational analysis we use the degeneracy-weighted center of gravity of the split lines.

We can combine the values of $\overline{B}'$, $\overline{B}''$ and $(\Delta A - \Delta\overline{B})$ determined from the analysis of the parallel transitions with the values of $(2K_a'' + 1)(A' - \overline{B}')$ from the perpendicular transitions to determine unique estimates for $\overline{B}', \overline{B}'', A', A''$. The last step in obtaining a set of approximate rotational constants is the application of the planar relationship[14]

$$C^{-1} = A^{-1} + B^{-1} \quad (2)$$

to determine values of C' and C''.

Once approximate constants and initial assignments of transitions are available, direct comparison of rigorously calculated asymmetric top rotational levels and the observed transition frequencies was made. Graphical simulations of the vinoxy rotational structure were obtained using a program originally written by Pierce.[15,16] The program generates the rotational energy levels for an asymmetric top by diagonalization of the asymmetric rotor Hamiltonian matrix in the symmetric top basis set. Ground state rotational level

TABLE II. Rotational constants and band origins for the vinoxy $\tilde{B}\,^2A'' - \tilde{X}\,^2A''$ system.

Band[a]	0, 0, 0[b]	1, 0, 0[b]	0, 1, 0[b]
A'	2.103 ± 0.004	2.03 ± 0.39	2.104 ± 0.004
B'	0.3442 ± 0.0012	0.3457 ± 0.0017	0.3441 ± 0.0020
C'	0.2958 ± 0.0012	0.2953 ± 0.0017	0.2957 ± 0.0020
κ'	...	...	± 0.057 ± 0.005[c]
A''	2.228 ± 0.012	2.14 ± 0.38	2.210 ± 0.012
B''	0.3809 ± 0.0010	0.3832 ± 0.0014	0.3823 ± 0.0018
C''	0.3253 ± 0.0010	0.3250 ± 0.0014	0.3259 ± 0.0018
κ''	...	...	± 0.025 ± 0.007[c]
T_{ov}	28 784.09 ± 0.01	29 701.24 ± 0.01	29 905.77 ± 0.01
# of lines fitted	46	31	53
J range	0–9	0–7	0–8
K_a range	0–2	0–2	0–5

[a] All bands originate from $v'' = 0, 0, 0$.
[b] Errors are one standard deviation.
[c] Arguments are presented in the text favoring the plus sign.

populations were calculated by assuming a Boltzmann distribution and the rotational line strengths were derived from the transformation matrices. The approximate constants were used to simulate the vinoxy spectrum and the result was close agreement between the observed and calculated spectra, in terms of both line positions and relative intensities. Unambiguous assignment of the majority of the observed lines was then made by direct comparison between the observed and calculated spectra.

Once a complete assignment had been achieved, the accurate rotational constants were determined by nonlinear least squares fitting to the line positions. A variation of the abovementioned program was used for this purpose, and the data for each vibrational level were treated separately. Initially the program was allowed to vary the band origin and all three rotational constants for both states. The inertial defects obtained from these fits were small (< 0.001 cm^{-1}) compared to the uncertainties in the rotational constants ($A \pm 0.01$ cm^{-1}, B and $C \pm 0.001$ cm^{-1}) showing that within experimental error, the molecule is planar in both states. Consequently, the data were refit by allowing only the band origin and the A and B constants to vary. In each fitting iteration the C constants were calculated from the planar relation [Eq. (2)]. Constraining the fits in this way significantly improved the standard deviations of the parameters obtained, mainly because of the reduced correlation in the five parameter fit. Rotational constants obtained from this procedure are listed in Table II. The standard error between the fitted and experimental line positions is ± 0.02 cm^{-1}, well within the observed spectral linewidth of ± 0.05 cm^{-1}. Correlation between pairs of constants such as B' and B'' is the major source of uncertainty in determining their absolute values. Differences between correlated pairs are derived with far greater accuracy than the constants themselves.[3] This problem is particularly evident in the analysis of the 1, 0, 0 band. Only $\Delta K_a = 0$ transitions were observed in this instance and as a consequence the A constants are extremely correlated producing a high degree of uncertainty in the fitted values.

To illustrate the quality of the fits we show in Fig. 7(b) a simulation of the spectrum of the 0,1,0 band which was generated using the constants from Table II and a temperature of 10 K. Comparison with the observed spectrum [Fig. 7(a)] shows excellent agreement.

C. Spin-rotation interaction

Since the vinoxy radical is an open-shell doublet state, (electronic) spin splittings might be expected in the spectrum. The general form of the spin-rotation Hamiltonian for a doublet asymmetric top was presented by Van Vleck[17] and contains six spin-rotation parameters for each electronic state. However, our measurements of the spin splittings are of relatively low precision and since vinoxy is very nearly a prolate symmetric top, it seems reasonable to neglect Hamiltonian terms which do not contribute matrix elements diagonal in K_a. (For $K_a = 1$, elements with $\Delta K_a = 2$ would connect nearly degenerate levels, but in the observed spectrum the $K_a = 1$ levels do not show observable spin splittings and so are not included in our data set.) In this case the spin-rotation Hamiltonian reduces to [18,19]

$$\mathsf{H}_{SR} = -a_0 \mathbf{N}\cdot\mathbf{S} - a[2N_zS_z - N_xS_x - N_yS_y] \quad (3)$$

which can be rewritten as

$$\mathsf{H}_{SR} = \mu \mathbf{N}\cdot\mathbf{S} + \kappa N_zS_z \quad (4)$$

where

$$\mu = a - a_0, \quad (5a)$$

$$\kappa = -3a. \quad (5b)$$

Taking the expectation value of H_{SR} in a prolate symmetric top basis yields the following formulas for the spin doublets[14,19]

$$F_1(N, K) = F_0(N, K) + 1/2\left(\kappa\frac{K^2}{N(N+1)} + \mu\right)N, \quad (6a)$$

$$F_2(N, K) = F_0(N, K) - 1/2\left(\kappa\frac{K^2}{N(N+1)} + \mu\right)(N+1), \quad (6b)$$

where $F_0(N, K)$ is the rotational term value without spin; F_1 and F_2 are the term values for $J = N + 1/2$ and $J = N - 1/2$, respectively; κ and μ are the spin-rotation coupling constants which are defined by Eqs. (5) in terms of the van Vleck parameters. As is well known, these parameters contain both first and second order contributions. Curl[20] gives formulas

for both contributions. His explicit results are for the Cartesian tensor components but they can be related to the Van Vleck spherical components via Table I in Curl and Kinsey.[21]

Spin-rotation coupling constants were determined by a nonlinear least squares fit of the splittings as predicted by Eqs. (6) to the measured line separations. Fits which involved variation of all four parameters were severely correlated and the μ values obtained were not statistically significant. When the μ constants were set to zero, a fit well within the experimental error limits was obtained giving $\kappa' = 0.057 \pm 0.005$ cm^{-1} and $\kappa'' = 0.025 \pm 0.007$ cm^{-1}.

Since these fits were to the observed splittings, only the relative signs of the spin-splitting constants κ are determined by this procedure. To determine the overall absolute sign we resort to two independent procedures. The F_1 levels are $2(N+1)$ degenerate, while the F_2 levels are only $2N$ degenerate, thus the F_1 transition should be slightly more intense. Similarly, using Eqs. (6) and remembering the theorem of spectroscopic stability, we recognize that if the F_1 component is shifted (from the position for the purely rotational transition) by an amount δ, then the F_2 component is shifted by an amount δ', where $\delta' = (N + 1/N)\delta$. Our previous rotational analysis allows accurate predictions of the purely rotational transition frequencies. While both the intensity and frequency asymmetry are small, they can be discerned for several spin-split transitions. These asymmetries in frequency and intensity favor an absolute positive sign for κ'' and κ'.

IV. DISCUSSION

The combination of the vibrational data in Table I and the rotational constants in Table II gives us considerable information about the electronic and geometric structure of vinoxy. This is especially true when combined with the *ab initio* calculations, especially those of Dupris *et al.*[3] The most important result from Table I is the dramatic decrease in the ν_1 vibrational frequency, nominally the CO stretch, in going from the ground $^2A''$ to the excited $^2A''$ state.

In the multiconfigurational calculation of Dupris *et al.*, it is found that the ground A'' state of vinoxy is about halfway between the ethenyloxy and formyl methyl resonance structures (see Fig. 1). The most important change in the electronic structure going to the excited A'' state is the promotion of approximately half an electron (in terms of occupation numbers) from a bonding C–C–O natural orbital to an antibonding one. Clearly, this is consistent with a distinct weakening of the C–O bond as reflected by the sharp drop in the ν_1 vibrational frequency.

The experimentally determined rotational constants give us more information about vinoxy. Because of the planarity of vinoxy only two independent rotational constants, i.e., A and B, are determined for each state. Unfortunately there are nine independent internal coordinates in vinoxy, so the structure cannot be uniquely determined from our experimental information alone. Clearly, the most significant internal coordinates are the C–C and C–O bond lengths and the C–C–O bond angle. The hydrogen atoms, being so light, make only a minor contribution to the moment of inertia.

TABLE III. Structural parameter for the vinoxy radical skeleton[a].

	$\tilde{B}\,^2A''$	$\tilde{X}\,^2A''$
$R(C_2O)$[b, c]	1.337 ± 0.002 (1.397)	1.272 ± 0.002 (1.275)
$<(C_1C_2O)$[b, d]	129.5 ± 0.1 (121.5)	121.9 ± 0.1 (122.9)
$R(C_1C_2)$[c, e]	1.466	1.405

[a] Subscripts on the atoms refer to the numbering in Fig. 2.
[b] Experimentally determined values, numbers in parentheses are from the work of Dupris *et al.*
[c] Bond lengths are in Å.
[d] Bond angles are in degrees.
[e] Parameter value given in Ref. 3, the H bond lengths and angles were also fixed at the values calculated in Ref. 3, i.e., for the $\tilde{X}$ state, $R(C_1H_1) = 1.071$, $R(C_1H_2) = 1.070$, $R(C_2H_3) = 1.078$, $<(H_1C_1C_2) = 120.2$, $<(H_2C_1C_2) = 120.5$, $<(H_3C_2C_1) = 117.8$; for the $\tilde{B}$ state $R(C_1H_1) = 1.069$, $R(C_1H_2) = 1.069$, $R(C_2H_2) = 1.069$, $<(H_2C_1C_2) = 120.0$, $<(H_2C_1C_2) = 119.5$, $<(H_3C_2C_1) = 120.9$.

Examination of the geometries calculated by Dupris *et al.*[3] shows that the hydrogens are bonded at distances and angles typical for bonding to sp^2 hybridized carbon atoms (cf. Table III). Electronic excitation has very little effect on the CH bonds because it basically involves the π orbitals. In view of these considerations, the calculated positions for the hydrogen atoms can be assumed.

Selection of the skeletal coordinate to be fixed is more difficult. The work of Dupris *et al.*[3] shows that electronic excitation has a large effect on the C–O bond, so we have chosen to assume the calculated C–C bond lengths and use the experimental rotational constants to obtain values for the C–O bond lengths and C–C–O bond angles. The results are given in Table III, along with the theoretical results which are reproduced for comparison. For the ground state the agreement between theory and experiment is excellent. Nonetheless it should be pointed out that the two bond lengths are not independent. Changing the C–C bond will cause a compensating change in the C–O bond length. The bond angle, however, is rather independently determined.

The measured parameters for the excited state are significantly different from the calculation, with the experimental bond length shorter, and the bond angle increased. These changes are necessary to account for the small moment of inertia observed about the a axis. This result is not an artifact of fixing the C–C bond length, the A' constant is very sensitive to the C–C–O angle. Reduction of the angle to 122° requires an unreasonable shortening of the C–O bond length to 0.97 Å and lengthening of the C–C bond to 1.85 Å. The theoretical value for the C–C bond length of 1.466 Å is very reasonable when compared against the C–C bond length of 1.50 Å in acetaldehyde (CH_3CHO). Similarly, the experimentally determined C–O bond length of 1.337 Å compares well with the C–O bond length of 1.36 Å for vinyl alcohol (CH_2CHOH). We therefore consider that the bond lengths and angles given in Table III represent an optimum combination of the experimental and theoretical data.

It is unlikely that any significant error is introduced

into the geometric determinations by assuming the H bond lengths and angles. However, it would be appealing to have a completely experimental determination of the C–C–O skeletal bond lengths and angles. Isotopic substitution could provide the required information. Work on deuterated samples is now underway, but is difficult due to the large amount of precursor needed in the production of vinoxy.

The remaining molecular parameter determined in the experiment is the spin-splitting parameter κ. It may at first be surprising that only κ and not μ is determined experimentally. However in the three doublet polyatomic molecules NH_2, ClO_2, and NO_2, for which there appear to be similar spin-splitting data,[19] the value of μ is usually at least an order of magnitude smaller than κ. This likely reflects the fact that μ is the difference [see Eq. (5)] between two quantities of similar magnitude.

The second order contribution to κ is caused by cross terms between the rotational uncoupling and the generalized spin-orbit coupling and is almost certainly the dominant contribution.[20] It is difficult to give a very precise interpretation of κ because of its second order nature. However, the fact that κ has the same sign in both the ground and excited $^2A''$ states implies that the intermediate $^2A'$ states does not dominate the interaction.

The observed spectral line positions for the low resolution excitation spectrum, laser excited, wavelength resolved emission spectrum, the rotationally resolved spectra, and the spin splittings are given, respectively, in Appendices A, B, C, and D. This material is available from the Physics Auxiliary Publication Service.[22]

ACKNOWLEDGMENTS

We would like to thank Professor David Gutman for originally bringing this problem to our attention and Professor Donald Levy for providing copies of the programs used for the rotational analysis. This work was supported, in part, by the ACS Petroleum Research Fund, Grant No. 14406-G6.

[1] K. Kleinermanns and A. C. Luntz, J. Phys. Chem. **85**, 1966 (1981).
[2] R. Buss, R. Baseman, G. He, and Y. T. Lee, J. Photochem. **17**, 389 (1981).
[3] M. Dupris, J. J. Wendoloski, and W. A. Lester, Jr., J. Chem. Phys. **76**, 488 (1982).
[4] N. C. Baird and K. F. Taylor, Can. J. Chem. **58**, 733 (1980).
[5] N. C. Baird, R. R. Gupta, and K. F. Taylor, J. Am. Chem. Soc. **101**, 4531 (1979).
[6] H. E. Hunziker, H. Kneppe, and H. R. Wendt, J. Photochem. **12**, 377 (1981) and H. E. Hunziker, H. Kneppe, A. D. McLean, P. Siegbahn, and H. R. Wendt, Can. J. Chem. **61**, 993 (1983).
[7] G. Inoue and H. Akimoto, J. Chem. Phys. **74**, 425 (1981).
[8] M. E. Jacox, Chem. Phys. **69**, 407 (1982).
[9] M. C. Heaven, T. Sears, V. E. Bondybey, and T. A. Miller, J. Chem. Phys. **75**, 5271 (1981) and M. Heaven, T. A. Miller, and V. E. Bondybey, *ibid.* **80**, 51 (1984).
[10] T. A. Miller, Science **223**, 545 (1984).
[11] B. A. Palmer, R. A. Keller, and R. Engleman, Los Alamos Laboratory Report, LA-825-MS, 1980.
[12] S. Gerstenkorn and P. Luc, *Atlas du Spectre D'Absorption de la Molecule D'Iode* (CNRS, Paris, 1978).
[13] G. R. Harrison, *MIT Wavelength Tables* (MIT, Cambridge, 1969).
[14] G. Herzberg, *Electronic Spectra and Electronic Structure of Polyatomic Molecules* (Van Nostrand Reinhold Company, New York, 1966).
[15] L. Pierce (unpublished).
[16] See C. A. Haynam, D. V. Brumbaugh, and D. H. Levy J. Chem. Phys. **79**, 1581 (1983) for the application of the program in the form used in this paper.
[17] J. H. Van Vleck, Rev. Mod. Phys. **23**, 213 (1951).
[18] R. S. Henderson, Phys. Rev. **100**, 723 (1955).
[19] W. T. Raynes, J. Chem. Phys. **41**, 3020 (1964).
[20] R. F. Curl, Jr., Mol. Phys. **9**, 585 (1965).
[21] R. F. Curl, Jr. and J. L. Kinsey, J. Chem. Phys. **35**, 1758 (1961).
[22] See AIP document no. PAPS JCPSA 81-2339-8 for 8 pages of Tables. Order by PAPS number and journal reference from American Institute of Physics, Physics Auxiliary Publication Service, 335 East 45th Street, New York, NY 10017. The price is $1.50 for each microfiche (98 pages) or $5.00 for photocopies of up to 30 pages, and $0.15 for each additional page over 30 pages. Airmail additional. Make checks payable to the American Institute of Physics.